THE JOURNAL OF PHYSICAL CHEMISTRY C
A JOURNAL OF THE AMERICAN CHEMICAL SOCIETY

pubs.acs.org/JPCC Article

Compressive Stress and Charge Redistribution during CO Adsorption onto Pt

David Raciti,* Kathleen A. Schwarz, John Vinson, and Gery R. Stafford

Cite This: *J. Phys. Chem. C* 2022, 126, 4446−4457 Read Online

ABSTRACT: The change in surface stress associated with the adsorption and oxidative stripping of carbon monoxide (CO) on (111)-textured Pt is examined using the wafer curvature method in 0.1 mol/L $KHCO_3$ electrolyte. The curvature of the Pt cantilever electrode was monitored as a function of potential in both CO-free and CO-saturated electrolytes. Although CO adsorbs as a neutral molecule, significant compressive stress, up to −1.3 N/m, is induced in the Pt. The magnitude of the stress change correlates directly with the CO coverage and, within the detection limits of the stress measurement, is elastically reversible. Density functional theory calculations of a CO-bound Pt surface indicate that charge redistribution from the first atomic layer of Pt to subsurface layers accounts for the observed compressive stress induced by the charge neutral adsorption of CO. A better understanding of adsorbate-induced surface stress is critical for the development of material platforms for sensing and catalysis.

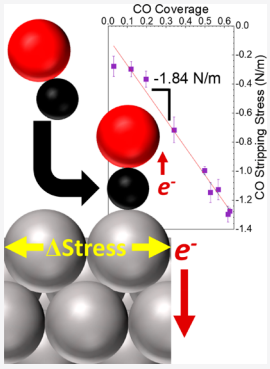

1. INTRODUCTION

Electro-organic reactions, where energy is either stored or released from chemical bonds within carbon-based molecules, are essential to help achieve a circular carbon-based economy.[1,2] Central to the electrochemical conversion of organic molecules is carbon monoxide (CO), which serves as both an intermediate in electrochemical CO_2 reduction to hydrocarbons and electrochemical oxidation in fuel cells that operate via oxygenated hydrocarbons (e.g., ethanol, methanol).[3,4] For the latter, Pt has been the predominant catalyst of choice, and substantial effort has been spent to identify the mechanistic details for the complete oxidation of alcohol-based fuels. With CO conversion serving as an important if not rate-limiting step of the oxidative process, it is critical to understand the state of a catalytic surface when CO is present.

The adsorption of CO is a purely chemical step that is generally irreversible. The CO-Pt binding energy of 96.5 kJ/mol is rather small compared to the 1072 kJ/mol dissociation energy of the CO triple bond[5,6] but is larger than most competitive adsorbates (such as H) and will readily displace such species from the Pt surface.[7,8] The binding of CO to Pt is understood in terms of the Blyholder model where only the highest occupied molecular orbital (HOMO) and lowest unoccupied molecular orbital (LUMO) of the molecule are involved in the bonding.[5,9−11] In this model, the bonding is derived from two contributions: the 5σ donation and 2π back-donation. Although there is significant electron interaction, the net charge transfer is quite low, supporting the experimental findings that CO adsorbs as a neutral molecule.[12]

The adsorption of CO as a neutral molecule should induce little surface stress change in the substrate; however, significant compressive stress has been measured for CO on Pt, adsorbed both electrochemically[13,14] and from the gas phase.[15] First-principles calculations also predict significant compressive stress associated with CO adsorption onto Pt.[13,16] Ibach has proposed a charge redistribution model, which argues that the sign of the adsorbate-induced surface stress should depend on the direction of the charge transfer that is involved in the formation of the surface bonds.[17] Electron-donating adsorbates, such as Cs on Ni(111), increase tensile stress because the electrons they donate to the outer metal layer strengthen in-plane bonds, while electron-withdrawing adsorbates, such as halides on Au, relieve tensile stress. However, this simple correlation lacks generality in that theoretical and experimental results clearly show that the adsorption of both H and O relieves the tensile stress on the Pt(111) surface,[18−21] even though O adatoms polarize charge away from the substrate, while H polarizes charge toward the substrate.

In this work, we explore the dynamic stress behavior associated with CO adsorption onto Pt in 0.1 mol/L $KHCO_3$ electrolyte. This was done via two independent stress measurement platforms using cantilever curvature measurements. The curvature of a Pt cantilever electrode was monitored as a function of potential in both CO-free and CO-saturated electrolytes. Stripping voltammetry was used to

Received: January 7, 2022
Revised: February 14, 2022
Published: February 24, 2022

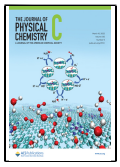

https://doi.org/10.1021/acs.jpcc.2c00134
J. Phys. Chem. C 2022, 126, 4446−4457

quantify the corresponding CO coverage. This allowed us to determine the adsorbate-induced biaxial stress vs CO coverage and guided subsequent computational simulations of charge redistribution mechanisms. Computational simulations predict that interactions between surface and subsurface atomic layers of Pt may be the source of the compressive stress induced by CO adsorption.

2. METHODS

2.1. Electrochemical Measurements. The electrolyte for all experiments was 0.1 mol/L $KHCO_3$ prepared by sparging 0.05 mol/L K_2CO_3 solution (Alfa Aesar, Puratronic#) with 20 sccm CO_2 overnight. Ultrapure water (18.3 MΩ-cm, Hydro, Picopure UV Plus) was used throughout the study. The pH of the as-prepared solution was 9.5. The electrochemical cell was an airtight single-compartment borosilicate cell sealed by an o-ring and Teflon cap. A glass disk was joined to the back of the cell to allow it to be held and positioned by a standard mirror mount on the optical bench. A full description of the cell is given elsewhere.[22] For these CO experiments, the cell was modified by inserting compression fittings into the Teflon cap to accommodate three poly(tetrafluoroethylene) (PTFE) tubes (0.8 mm ID, 1.6 mm OD) to serve as a Luggin capillary, a gas purge line, and a separate gas return line. The Luggin capillary and purge line were inserted into the electrolyte, while the return line was positioned in the headspace of the cell. The Luggin capillary was filled with 1.0 mol/L $KHCO_3$ and contained a fine "leakless" frit at the end to prevent leakage into the electrolyte. Gas flow was controlled by a mass flow controller (Alicat Scientific) with separate feed lines for argon (Ar) and carbon monoxide (CO). Working with CO is hazardous; any experiments with CO were conducted with verified gas-tight equipment in rooms equipped with several CO monitors including personal CO monitors for users. The counter electrode was a Pt screen placed parallel to the cantilever working electrode. The reference electrode was the saturated mercury/mercurous sulfate (SSE) and was placed outside of the electrochemical cell but was connected to the electrolyte by the fritted Luggin capillary. Potentials are referenced to SSE, except where specified. Potential control was maintained using an EG&G Princeton Applied Research Corp. model 273 potentiostat−galvanostat controlled by in-house LabView software. All measurements were made at room temperature.

2.2. *In Situ* Curvature Measurements and Cantilever Fabrication. *In situ* stress measurements were made on a vibration-isolating optical bench using the cantilever bending method. The cantilever was a Si ⟨100⟩ (WRS Materials) strip measuring 60 mm × 3.8 mm × 0.115 mm. Young's modulus and Poisson ratio of the Si were 130×10^9 N/m^2 and 0.28, respectively. A 6 nm thick adhesion layer of titanium (Ti) and a subsequent 90 nm film of platinum (Pt) were sputtered onto one side of the cantilever. The (200) reflection was completely absent in X-ray diffraction patterns (Figure S1 inset), and the (111) rocking curve typically had a full width at half-maximum of 4.8° indicative of a strong (111) crystallographic orientation.[23] Based on the curvature of the cantilever in air following sputtering, the Pt was under compressive stress. The electrochemically active surface area (roughness factor), as determined by hydrogen adsorption/desorption was 1.05. A typical voltammogram is shown in the Supporting Information (SI), Figure S1. The top portion of the cantilever was masked with vinyl electroplating tape (3 M) to expose a cantilever length of 25 mm. The curvature of the substrate was monitored while in the electrolyte and under potential control. The relationship between the force per cantilever beam width, ΔF_w, exerted by processes occurring on the electrode surface and the curvature change ($\Delta\kappa$) induced in the cantilever is given by Stoney's equation[24]

$$\Delta F_w = \frac{Y_s h_s^2 \Delta\kappa}{6(1-\nu_s)} \tag{1}$$

where Y_s, ν_s, and h_s are Young's modulus, Poisson ratio, and thickness of the Si substrate, respectively. The initial value of ΔF_w is arbitrarily set to zero at the beginning of the measurement. Since only surface processes are examined in this paper, we will refer to ΔF_w as the change in surface stress and designate it as Δf.

Two *in situ* methods were used to monitor the curvature of the cantilever electrode. The first reflects a 1 mW HeNe laser off of the polished Si side of the cantilever and onto a position-sensitive detector (PSD). A small-angle approximation was used to estimate the curvature of the Si cantilever directly from the reflected laser position on the PSD. A more detailed description of this optical bench and methods used for estimating the curvature are published elsewhere.[25,26] The advantage of this system is the speed at which the stress data can be collected. Collection speeds of 500 Hz have been reported,[27] but in this study, stress data is typically collected at 50 Hz. The second advantage of this system is the high surface stress resolution. Surface stress changes of 10^{-3} N/m can typically be resolved from cantilever electrodes while in solution.[26] The disadvantage of this system is that a single, stationary laser measures only the change in curvature, rather than absolute curvature, by measuring the change in position of the reflected beam. It also interprets all cantilever movement as a change in curvature, i.e., stress. This makes stress measurements under the gas bubbling conditions used here extremely challenging. For this reason, the single laser system was primarily used in voltammetric and potential pulse experiments where the solution was quiescent, and the measurement time was short enough to negate the influences of drift.

A multibeam optical stress sensor (MOSS), similar to that described in previous studies,[28−30] was also used to measure cantilever curvature. This apparatus consists of an 18 mW AlGaInP (658 nm) diode laser, an etalon that generates three parallel laser beams, a beam splitter, mirrors, servos for mirror control, and a CCD video camera. The change in cantilever curvature, $\Delta\kappa$, is given by

$$\Delta\kappa = \frac{(D - D_i)}{D_o}\frac{\cos(\alpha)}{2L} \tag{2}$$

where D is the average spacing between adjacent laser spots reflected onto the CCD camera, D_i is the average initial spacing, D_o is the spacing between the parallel incident beams, L is the distance between the cantilever and CCD, and α is the angle of incidence (typically equal to zero). D_o was determined prior to the experiment by replacing the electrochemical cell with a flat mirror. Spot coordinates on the CCD were determined using Vision Builder (National Instruments) image processing software and LabView. Two computer-controlled servos (Kinesis) center the laser spots onto the CCD to negate laser drift. Potential control was maintained using a Biologic SP-200 potentiostat and EC-Lab software. The typical stress

https://doi.org/10.1021/acs.jpcc.2c00134
J. Phys. Chem. C 2022, 126, 4446−4457

resolution with this system is approximately 0.06 N/m, a factor of 60 less than the single laser deflection system. In addition, due to the mirror servos, data acquisition is reduced to 0.5 Hz. The primary advantage of the MOSS system is that the measurement tends to be less sensitive to vibrations. If the three laser spots are impacted equally, the spot locations change, but the distance between the spots (ΔD) remains unchanged.

For the reasons discussed above, the MOSS was used to measure the steady-state stress associated with CO adsorption and electrochemical stripping from Pt cantilever electrodes. Stress measurements were made only in the absence of gas bubbling. The electrolyte was first deaerated with Ar at a flow rate of 15 mL/min for 1 h while the potential was set to the desired value for CO adsorption, E_{ads}. Gas flow was stopped, and the initial curvature of the cantilever was measured using the MOSS. A typical measurement was made for 2 min and consisted of about 60 data points. CO was then introduced into the cell at a flow rate of 3 mL/min. Saturation, a concentration of approximately 1 mmol/L, was achieved in 10 min. Gas flow was stopped, and a second curvature measurement was made. The difference represents the stress change for CO adsorption at E_{ads} in equilibrium with a CO-saturated solution. Ar was then bubbled at a rate of 15 mL/min to flush the CO from solution. A third curvature measurement was made, representing the stress change for CO adsorption at E_{ads} when CO is absent from the electrolyte. The adsorbed CO was then electrochemically stripped from the Pt while the charge and stress change were measured.

Although the curvature measurements were made in the absence of gas flow, to associate the curvature change with CO adsorption, one must assume that curvature was not affected by gas bubbling. This assumption was tested for the two flow rates used during a typical CO adsorption cycle at a fixed potential of −0.2 V vs SSE. The results, discussed in the SI (see the Uncertainty in Curvature Measurement during Gas Bubbling section and Figure S2), generate an overall uncertainty in the measurement, given by the following expression

$$\varepsilon_T = ((\sigma_i + \sigma_f)^2 + \varepsilon_b^2)^{1/2} \quad (3)$$

where ε_T is the total uncertainty in the measurement, σ_i and σ_f are the standard deviations of the initial and final stress measurements, respectively, and ε_b is the average error introduced by gas bubbling, as shown in Figure S2. The ε_b values used were 0.02 and 0.06 N/m for flows of 3 and 15 mL/min, respectively. The ε_T values are represented as error bars in the stress plots.

2.3. Computational Details. We performed density functional theory (DFT) calculations within the generalized gradient approximation (GGA) to find the stress of Pt(111) and Pt(111) with 0.25 monolayer (ML) CO in the atop position. All calculations used Quantum Espresso, version 6.7 GPU, with a plane-wave cutoff of 120 Ry, the Perdew−Burke−Ernzerhof (PBE)[31] exchange−correlation potential, and Pseudo-Dojo pseudopotentials (C.upf, O-high.upf, Pt-sp.upf)[32,33] generated with ONCVPSP 3.3.1.[34] The unit cell had 6 Pt layers and was sampled with a 6 × 6 × 1 k-point mesh (1 1 0 offset). To prevent spurious interactions, we applied the vacuum effective screening medium (ESM) method boundary condition and used a cell height of 70 Bohr cell.[35] We find our value of 4.79 N/m for the Pt(111) surface stress in good agreement with GGA calculations from the literature.[13,36] Additionally, Ha et al. report a 1/4 ML CO coverage stress of −1.55 N/m, also for a 6 Pt layer unit cell.[13] We find our value of −1.65 N/m in good agreement with these results. We note that these calculations are for CO binding to a clean Pt surface, and future work could include the contributions of water on the Pt surface.

3. RESULTS AND DISCUSSION

3.1. Electrochemical and Stress Response of Pt to CO. The rest potential of the Pt cantilever electrode in Ar-purged 0.1 mol/L $KHCO_3$ is near −0.115 V vs SSE. After 10 min of CO sparging to saturate the electrolyte, the rest potential shifts in the negative direction to −0.68 V, reflecting the adlayer of CO on the Pt surface. Figure 1 shows the voltammetry (a) and surface stress response (b) of the cantilever electrode with and without CO present in solution. In the absence of CO, the voltammetry is dominated by hydrogen adsorption/desorption at negative potentials and PtO formation/reduction at positive

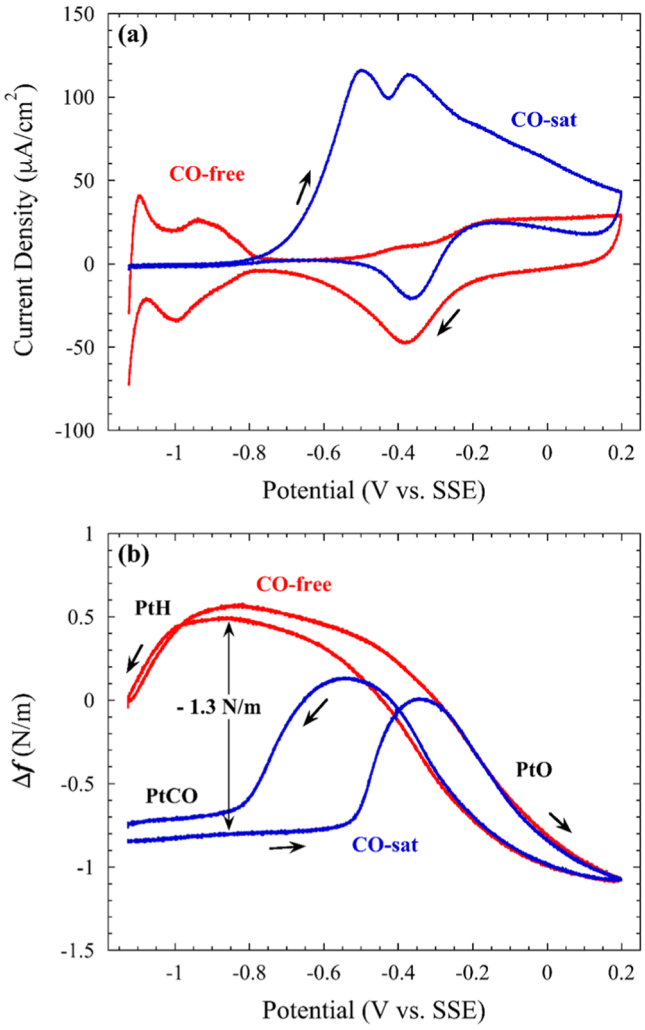

Figure 1. (a) Potentiodynamic scan and (b) surface stress response (Δf) of a (111)-textured Pt cantilever electrode in 0.1 mol/L $KHCO_3$, with (blue curve) and without (red curve) the CO-saturated electrolyte. Although Δf is arbitrarily set to 0 at the beginning of the experiment, the CO-sat stress curve in panel (b) was shifted along the stress axis to highlight the identical response with the CO-free curve in the PtO region. The sweep rate was 25 mV/s, and the solution pH was 9.5.

https://doi.org/10.1021/acs.jpcc.2c00134
J. Phys. Chem. C 2022, 126, 4446−4457

potentials. The stress is compressive in both regions and shows hysteresis associated with oxide formation. As expected, the stress response for hydrogen adsorption/desorption is fairly reversible. In the presence of CO, the voltammetry indicates that CO completely prevents hydrogen adsorption onto Pt due to the absence of the symmetric peaks between −1.1 and −0.8 V vs SSE in Figure 1a. In CO, as the potential is scanned in the positive direction, CO oxidation begins near −0.90 V/SSE and shows two current peaks at about −0.5 and −0.35 V. The two CO oxidation peaks are well positive of the standard potential for CO oxidation of −0.11 V vs RHE (≈−1.2 V vs SSE), which is partly due to the blocking nature of the CO adlayer, effectively preventing the water molecules, necessary for CO oxidation, from reaching the Pt surface.[37,38] The higher anodic current in the CO-saturated electrolyte following CO stripping (Figure 1a) is due to the bulk oxidation of CO in solution.

The oxidation of adsorbed CO follows the Langmuir−Hinshelwood mechanism,[39] where the adsorbed CO reacts with the adjacently adsorbed oxygenated species

$$\mathrm{Pt-CO + Pt-OH \rightarrow 2Pt + CO_2 + H^+ + e^-} \quad (4)$$

leaving two open Pt sites where anion adsorption can follow. On polycrystalline Pt electrodes in acidic electrolyte, the primary CO oxidation peak often appears as two peaks, like that shown in Figure 1a, when CO is adsorbed at $E_{ads} \leq 0.3$ V vs RHE. The two peaks likely correspond to the oxidation of CO adsorbed on different surface sites, which is supported by corresponding FTIR spectra.[37] The latter peak alone is observed for $E_{ads} \geq 0.3$ V vs RHE. In 0.1 M NaOH electrolyte (pH 13), CO oxidation begins at more negative potentials than in acidic solution and exhibits three oxidation peaks prior to Pt oxidation,[13] in contrast to what we observe in 0.1 M $KHCO_3$ (pH 9.5).

The stress response with and without CO in solution is shown in Figure 1b. The curves were adjusted along the stress axis to highlight the fact that the responses in the PtO region superimpose. The bulk oxidation of CO in solution has no stress signature, as noted by Ha et al.[13] The most striking feature when CO is present is the compressive stress change induced in the Pt cantilever by CO adsorption. As the potential is swept cathodically from the PtO region, CO adsorption begins at about −0.45 V, where the stress response begins to move in the compressive direction with respect to the curve for CO-free Pt. The adsorption of CO may even facilitate the reduction of PtO through its oxidation to CO_2.[40] A maximum stress difference of −1.3 N/m is seen at a potential of about −0.85 V. This represents the stress difference between an anion-covered Pt surface (at potentials approaching hydrogen adsorption) and the CO-covered Pt surface. The stress response due to hydrogen adsorption is completely absent on the CO-covered Pt surface, similar to the voltammetric response.

As the potential is swept in the anodic direction from −1.1 V, the stress moves very slightly in the tensile direction with no corresponding electrochemical response. Molecular orbital calculations for CO chemisorption on Pt suggest that an increase in anodic potential results in a decreased back-donation from Pt to the π^* level of CO.[41] This is in good agreement with experimental results showing a decrease in the Pt−C and an increase in the C−O stretching frequencies with increased anodic potential, as a result of weakening of the back-donation bond to the surface.[42] This increased surface charge density in the Pt can account for the observed tensile stress in this potential region. As the potential is further increased, an abrupt tensile increase is observed at about −0.5 V, about 0.3 V positive of initial CO oxidation, suggesting that the loss of loosely bound CO has little impact on the surface stress. The largest change in stress occurs at the voltammetric trough between the two current peaks. In this potential region, the stress responds to both the removal of CO and the adsorption of anions onto the Pt surface. Eventually, the stress becomes compressive and replicates the response for OH adsorption in the absence of CO in solution.

The rate and potential dependence of CO adsorption were examined by pulsing the potential from an initial value of −0.2 V, which is positive of the CO stripping potential but negative of PtO formation, to more cathodic potentials for 100 s and then returning the potential to −0.2 V. The results are shown in Figure 2. In the absence of CO (Figure 2a), normal electrocapillarity is observed. The stress response is tensile and stabilizes within the 100 s pulse. Both the addition of negative charge and anion desorption are expected to produce tensile stress, consistent with Ibach's charge redistribution model.[17] When the pulse potential reaches −0.9 V, there is a slight decrease in the stress due to the onset of hydrogen adsorption. This is clearly evident at −1.0 V where the postpulse stress fails to reach the values of the previous pulses and the stress moves in the compressive direction at a rate that appears to be diffusion-controlled.

When CO is added to the electrolyte (Figure 2b), the tensile to compressive transition occurs ≈0.5 V more positive (between −0.4 and −0.5 V). A pulse potential of −0.4 V shows a slight downward deflection while the response for −0.5 V is clearly moving in the compressive direction. This continues for all pulse potentials examined negative of −0.4 V. Similar to the curve for hydrogen adsorption in Figure 2a, the stress should respond to the double layer charge from the potential step, followed by the adsorption of CO onto the Pt surface. The CO can influence the stress in several ways, by altering the charge density on the Pt surface (either by direct charge transfer or by causing a charge redistribution in the Pt), by shifting the potential of zero charge (pzc) of the Pt, and by adsorbate−adsorbate interactions when at high coverage.

Figure 2c shows a plot of the net stress change for pulses shown in Figure 2a,b. The magnitude of the stress change is similar for both pulse directions. In the CO-free electrolyte, the stress reaches a maximum tensile value at −0.9 V at which point compressive stress due to hydrogen adsorption comes into play. When CO is present, the compressive stress due to its adsorption begins just negative of −0.4 V. The fact that the stress response is the same in the −0.2 to −0.4 V range, whether CO is present or not, indicates that CO does not adsorb at these potentials. The shape of the curves in Figure 2c is quite similar to the cathodic stress response shown in Figure 1b. Compressive stress occurs at more positive potentials when CO is present in solution. The difference between the two sets of curves in Figure 2c at −0.9 V is about −1.28 N/m, which is nearly identical to the CO-induced stress obtained from the Figure 1b voltammetry at this potential.

The surface stress response to the potentiostatic pulses shown in Figure 2b suggests that CO coverage and the stress induced over the first 100 s of CO adsorption have a potential dependence in the range of −0.4 to −0.8 V. The stress levels off at more cathodic potentials. Ibach has examined the CO stress response on Pt(111) in UHV as a function of coverage and finds a linear relationship at low coverage where the stress

https://doi.org/10.1021/acs.jpcc.2c00134
J. Phys. Chem. C 2022, 126, 4446−4457

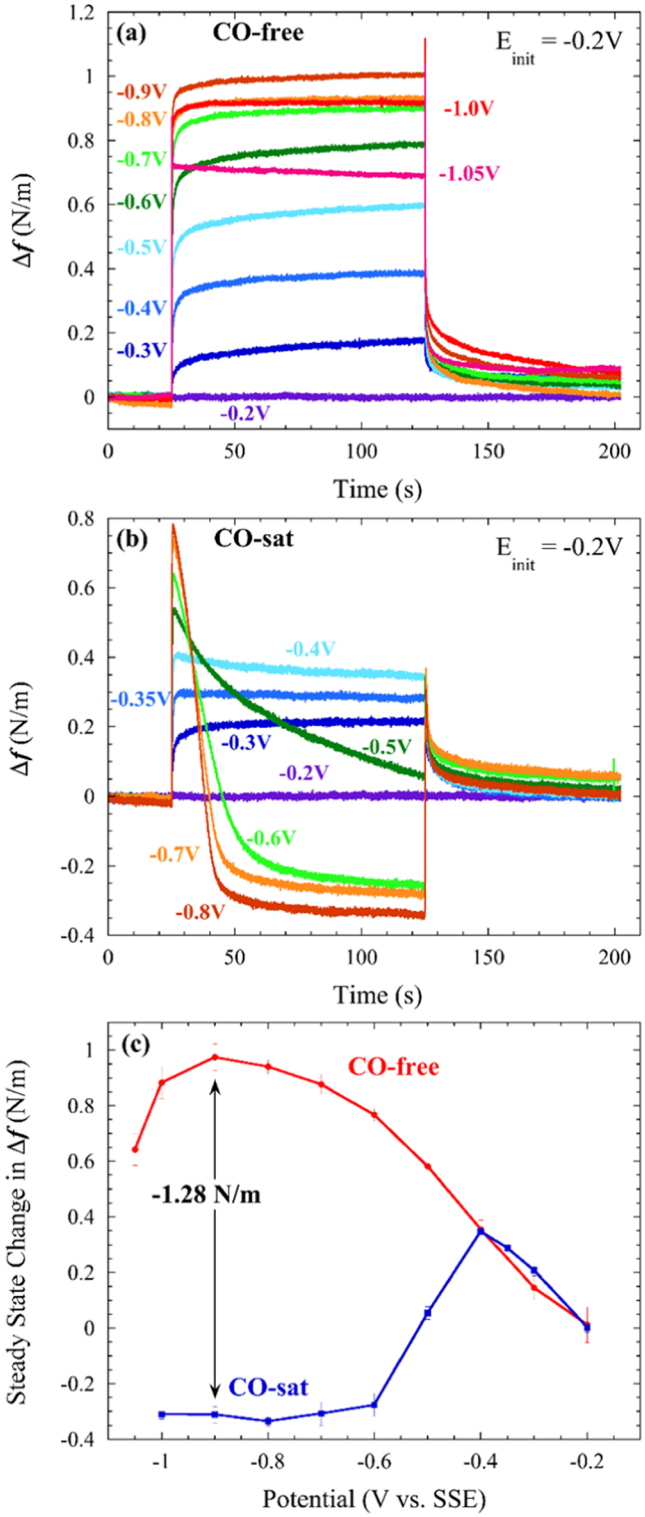

Figure 2. Surface stress response (Δf) of a (111)-textured Pt cantilever electrode to potentiostatic cathodic pulses from a starting potential of −0.20 V vs SSE in 0.1 mol/L $KHCO_3$ saturated with (a) Ar (CO-free) or (b) CO. The pulse duration was 100 s, followed by a return pulse to −0.20 V for 75 s. (c) The average net stress change for both cathodic and return pulses shown in panels (a) and (b).

is due to adsorbate−surface interactions.[15] At increased coverage, there is an additional compressive contribution due to adsorbate−adsorbate interactions. Similar nonlinear behavior has also been suggested through DFT calculations.[13] Although surface stress measurements have been made during the electrochemical adsorption of CO onto Pt, stress as a function of CO coverage has not been reported.[13,14]

3.2. Quantifying CO Coverage on Pt. The adsorption of CO is considered to be a purely chemical process, adsorbing as a neutral molecule, so its adsorption does not involve an electrochemically detectable charge transfer that can be used to quantify its coverage. This has been demonstrated in the literature by displacing an iodine layer on Pt(111)[12] whose structure and coverage are well known from STM.[43] The displaced charge density of −104 μC cm^{-2} is consistent with the calculated charge based on the iodine coverage. Stripping voltammetry is generally used to quantify the CO coverage through its 2-electron oxidation to CO_2. However, there is a discrepancy in coverage determined by this method and spectroscopic methods due to errors associated with double layer charging. We use a method developed by Clavilier[44] to determine CO coverage that has become widely used in the literature.[8,12,45−49] The electrolyte is first purged with Ar, and the potential is cycled between the platinum oxide and hydrogen regions to clean the Pt surface. The potential is then fixed at E_{ads} while CO is introduced. Once the CO layer is established, the system is purged with Ar for 30 min to remove the remaining CO from solution. The CO adlayer is then oxidized to CO_2 by sweeping the potential from E_{ads} to a potential where CO is completely oxidized, E_{ox}. The voltammetry is then repeated to generate a background response in the absence of CO on the surface.

Figure 3 shows a typical current and stress response to voltammetric stripping of a CO layer that had been adsorbed from the saturated solution at a fixed potential. The CO in solution had been removed by Ar purging prior to stripping the CO adlayer. Examples from both stress measurement techniques, discussed in Section 2.2 "*In situ* Curvature Measurements and Cantilever Fabrication", demonstrate that similar stress/potential profiles can be obtained for numerical evaluation. The initial voltammetric cycle (Figure 3a,c) shows the absence of hydrogen desorption as the potential is increased from E_{ads}. With a further increase in potential, the 2-electron oxidation of adsorbed CO to CO_2 appears as two separate current peaks. A single oxidation peak was observed, when stepping by 25 mV increments, for $E_{ads} \geq -0.7$ V (for example, see SI, Figure S3). The voltammetry in the Pt oxidation/reduction region is identical to the subsequent voltammetry in the absence of CO on the surface. An additional post-CO stripping CV, denoted as #3 in Figure 3a,b, is identical to CV #2, indicating that all CO, present in the system, was oxidized on the first cycle. Following CO stripping, hydrogen adsorption returns at potentials negative of −0.8 V. Although the characteristic features seen on clean Pt (Figure S1) are absent, they tend to return with continued cycling under an Ar purge. We also note that the hydrogen desorption charge from clean Pt and from freshly stripped Pt is essentially identical, suggesting that the CO cycle causes no significant area change to this particular Pt surface.

The corresponding changes in surface stress are shown in Figure 3b,d. The stress was arbitrarily set to zero at the beginning of the first voltammogram. Initially, the stress remains relatively constant during the potential sweep before increasing in the tensile direction as the CO is oxidized from the Pt surface. The stress does not reflect the apparent two separate CO oxidation peaks that appear in the voltammetry. As seen previously in the CO-saturated solution (Figure 1), the

https://doi.org/10.1021/acs.jpcc.2c00134
J. Phys. Chem. C 2022, 126, 4446−4457

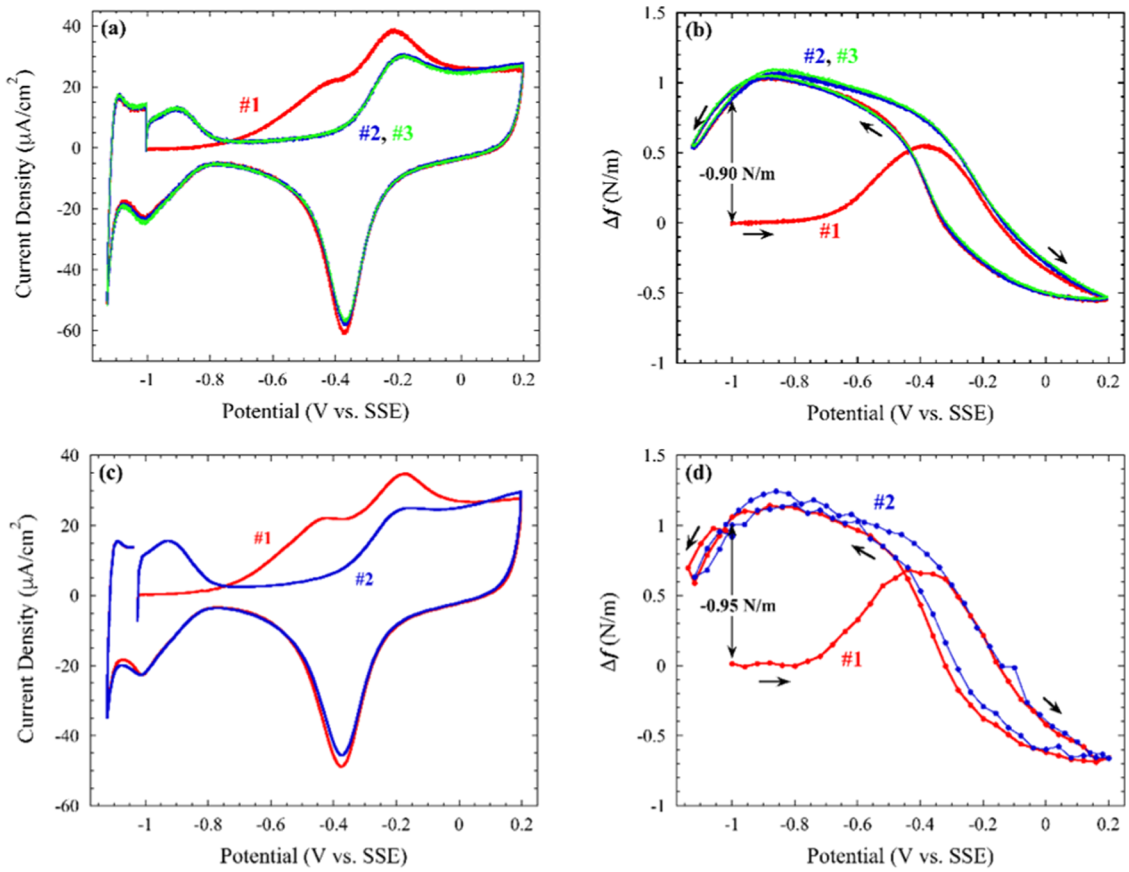

Figure 3. (a) Stripping voltammetry and (b) surface stress response (Δf) of a (111)-textured Pt cantilever electrode in CO-free 0.1 mol/L $KHCO_3$ following CO adsorption at $E = -1.0$ V from CO-saturated solution using a single-beam HeNe laser to estimate the cantilever curvature. (c) Stripping voltammetry and (d) surface stress response (Δf) of a (111)-textured Pt cantilever electrode in CO-free 0.1 mol/L $KHCO_3$ following CO adsorption at $E = -1.025$ V from CO-saturated solution using a MOSS to measure the cantilever curvature.

stress reaches its maximum at the trough between the two peaks, suggesting that OH^- adsorption becomes the dominant process as the potential is further increased. Upon reduction of the PtO, the stress once again becomes tensile before turning compressive again in the hydrogen adsorption region. Because CO is no longer present in solution, readsorption does not occur on the return sweep and the stress response is similar to that shown in Figure 1b for the CO-free electrolyte. It should be noted that once the CO is removed from the surface, the stress response is identical to the subsequent background response for Pt, again indicating that all CO has been removed during the stripping cycle. The CO-induced stress can be estimated from the stress difference at E_{ads}. In the cases provided here, a stress change of −0.90 N/m was measured from a CO layer adsorbed at $E_{ads} = -1.0$ V using the single HeNe laser, while a similar stress change of −0.95 N/m was measured from a CO layer adsorbed at $E_{ads} = -1.025$ V using the MOSS. These stress values do not represent the absolute stress induced by CO to the Pt surface; rather, it represents the difference between the stress state of a CO-covered Pt surface and a surface with mixed coverage of adsorbed hydrogen and anions that would normally be present on the surface at E_{ads} in CO-free solution.

Significant effort has been made to quantify the CO coverage electrochemically by means of stripping voltammetry with appropriate double layer corrections.[37,44−47] CO coverages determined from this technique are generally in line with those determined spectroscopically.[37,46] A series of electrochemical measurements must be made to capture the changes in double layer capacitance due to CO adsorption, as well as the charge contributions from anion adsorption/desorption. The charge associated with the entire sequence is

$$q_{CO,F} = q_T - (q_{dis} + q_b) \tag{5}$$

where $q_{CO,F}$ is the net faradic charge density for the two-electron oxidation of the CO adlayer to CO_2 and q_T is the total charge obtained from the initial voltammetric sweep from E_{ads} to E_{ox}, like that shown in Figure 3a,c (the CO stripping charge). The two additional terms in eq 5 consist of q_b, the background charge measured between E_{ads} and E_{ox} in the absence of the CO layer, and q_{dis}, the displacement charge measured at E_{ads} upon desorbing the CO adlayer. The quantity ($q_b + q_{dis}$) equals the overall charge density for double layer charging between E_{ads} and E_{ox} involving desorption of the CO adlayer without oxidizing it, whereas q_T refers to the same potential sweep but now including the faradic charge for converting adsorbed CO to CO_2. The value of q_b is obtained by integrating the voltammetric current measured in the absence of chemisorbed CO between E_{ads} and E_{ox}, i.e., the voltammogram(s) following CO stripping. The quantity q_{dis} reflects the fact that at E_{ads}, either hydrogen or anions are adsorbed onto the clean Pt surface once the CO has been removed; however, the quantity $-q_{dis}$ is generally obtained by examining the opposite process, i.e., the CO adsorption step. Although CO adsorbs as a neutral molecule, one observes a

https://doi.org/10.1021/acs.jpcc.2c00134
J. Phys. Chem. C 2022, 126, 4446−4457

current transient due to the displacement of the species already present on the surface prior to CO adsorption. Desorbed hydrogen is expected to produce a positive charge, while desorbed anions produce a negative charge. The potential at which the charge passes through zero is the potential of zero total charge (PZTC), an empirical quantity not to be confused with the PZC, a thermodynamic quantity. For polycrystalline Pt, the PZTC is reported to be +0.28 V vs RHE.[37] In addition to the displacement charge for species leaving the surface, one also measures charge due to changes in the double layer. Taken together, these contributions can be reliably captured for q_{dis}.

As an example, we have applied this technique to the voltammetry shown in Figure 3a. Integration of the stripping current from E_{ads} = −1.0 V to E_{ox} = + 0.20 V for the stripping and subsequent voltammogram yields a value of 243 μC/cm^2 for the quantity $q_T - q_b$. This quantity takes into account the 1.05 roughness factor of the Pt cantilever. Due to the slow CO flow rate required to obtain an accurate stress measurement, the long transition time for CO adsorption, nearly 600 s, makes it difficult to detect the displacement current from the background needed for q_{dis}. However, a study focusing on the potential dependence of q_{dis} at potentials negative of CO oxidation indicates that the difference between q_{dis} at two potential values is identical to integrating the background voltammogram between the same potential limits.[45] A plot of $-q_{dis}$ vs E_{ads}, obtained by this method and used in eq 5, is shown in the SI, Figure S4. An E_{PZTC} value of −0.80 V is obtained from the plot, very similar to that of −0.81 V (+ 0.28 V vs RHE) reported by Cuesta for polycrystalline Pt.[37] Going back to the Figure 3a example for CO adsorption at −1.0 V, $-q_{dis}$ is generated due to the oxidative displacement of H from the Pt surface. The value of $-q_{dis}$ obtained from Figure S4 at a potential of −1.0 V is 85 μC/cm^2. Adding $-q_{dis}$ to $q_T - q_b$ above results in a faradic charge for CO oxidation of 328 μC/cm^2, reflecting a CO coverage (θ) of 0.68 (normalized to the metal atomic density of 1.50×10^{15} atoms cm^{-2} for Pt(111)). This compares nicely to the maximum CO coverage of 0.68 reported for Pt(111) in the CO-free electrolyte.[37] The same procedure applied to Figure 3c yields a CO coverage of 0.69 for E_{ads} = −1.025 V.

3.3. Deriving CO Coverage from Stress Measurements. Measurements, similar to those shown in Figure 3c,d using the MOSS, were made over a potential range of −0.5 to −1.1 V to determine the stress change associated with CO adsorption in both CO-saturated and CO-free electrolytes, as well as the stress and charge associated with voltammetric stripping of the CO from the Pt surface. Figure 4 shows a plot of CO coverage as a function of adsorption potential, obtained from stripping voltammetry using the procedure outlined above. The CO coverage ranges from 0.73 at the most negative potential down to 0.04 as the adsorption potential moves in the positive direction. These values represent the CO coverage in the CO-free electrolyte. The solid line in the figure is simply a guide for the eye. An extrapolation of this line indicates that CO adsorption occurs at potentials negative of −0.4 V, consistent with the stress response to the potentiostatic pulses in Figure 2c. The observed decrease in CO coverage with increasing adsorption potential is somewhat more prominent than that reported over a similar potential range for polycrystalline Pt in 0.1 M $HClO_4$.[37] This might be due to the higher pH in 0.1 mol/L $KHCO_3$.[50]

The corresponding stress measurements are shown in Figure 5. As outlined in Section 2.2, the steady-state curvature of the cantilever was measured prior to introducing CO into the cell, following 10 min of CO purging at 3 mL/min and following 30 min of Ar purging at 15 mL/min. The curvature difference following the CO purge and the initial value represents the CO-induced stress for an adlayer in equilibrium with a CO-saturated solution. The curvature difference following the Ar purge and the initial value represents the CO-induced stress for an adlayer in CO-free solution. In addition to these steady-state stresses, the stress change associated with voltammetric stripping, as well as the stress obtained from the Figure 2 pulse experiments in the CO-saturated solution, are shown. Because the reference state for the voltammetric stripping measurements is the CO-free Pt surface at E_{ads}, the pulse data plotted in Figure 5 is the difference between the CO-saturated and

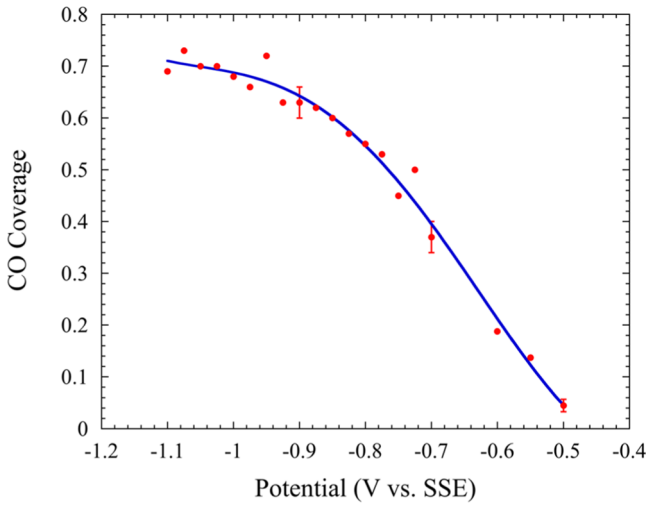

Figure 4. CO coverage as a function of potential for CO adsorption from CO-saturated solution followed by voltammetric stripping in CO-free 0.1 mol/L $KHCO_3$. Error bars represent the standard deviation for multiple measurements made at a given potential. The solid curve is a guide for the eye.

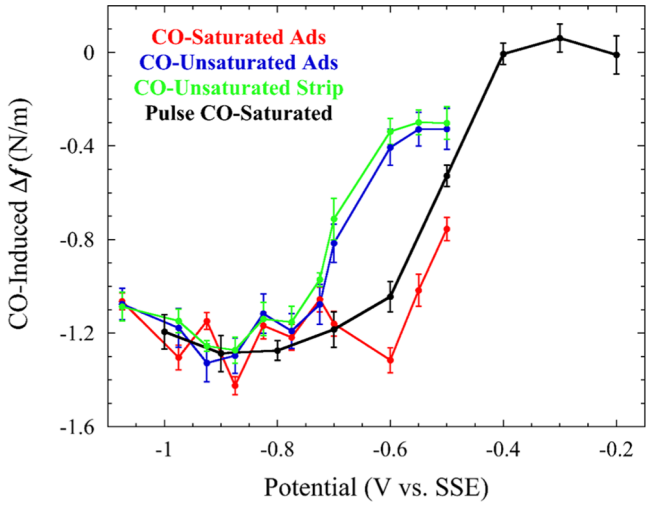

Figure 5. CO-induced surface stress change (Δf) measured by the MOSS during the CO adsorption cycle at fixed potential; following CO purging at 3 mL/min for 10 min (red), following Ar purging at 15 mL/min for 30 min to remove the CO from solution (blue), following surface CO removal by voltammetric stripping (green), and the difference between the CO-saturated and CO-free stress values obtained from the potentiostatic pulses shown in Figure 2c (black).

https://doi.org/10.1021/acs.jpcc.2c00134
J. Phys. Chem. C 2022, 126, 4446−4457

CO-free values plotted in Figure 2c. It is interesting to note that the pulse stress values and the steady-state adsorption values from the saturated solution are very similar, particularly at more negative potentials. The small discrepancy at more positive potentials may reflect a longer time required to reach equilibrium due to CO oxidation at these potentials. All four stress measurements give similar values at potentials negative of −0.8 V. The decrease in compressive stress as the potential approaches −1.1 V is not due to a loss of CO coverage but to an increase in hydrogen coverage of the Pt reference state (see Figure 2c). DFT calculations indicate that both a 1 × 1 monolayer of H and a full monolayer of CO (θ = 0.68) produce a stress of about −4.5 N/m.[13,18]

Cuesta has examined the equilibrium CO coverage on Pt(111) electrodes, held at E_{ads} = 0.1 V vs RHE, in 0.1 mol/L H_2SO_4 as a function of the CO partial pressure in equilibrium with the electrolyte. CO coverage was quantified using both stripping voltammetry and Fourier-transform infrared spectroscopy (FTIR). A maximum CO coverage of 0.75 was measured under saturated conditions. Under extremely low CO concentration, the equilibrium surface coverage drops to 0.68.[51] Although a similar decrease in the CO surface coverage should occur between the CO-saturated and CO-free electrolytes at the more negative potentials in Figure 5, the associated stress change falls within the uncertainty in the stress measurement. However, at more positive potentials, the two stress measurements made from CO-free solution deviate significantly from the CO-saturated measurements. Spectroscopic evidence for stable CO adlayers up to 0.9 V vs RHE in CO-saturated solutions has also been reported, whereas the onset of CO monolayer oxidation in CO-free solution is less positive by 220 mV.[52] It is encouraging to note that the adsorption stress from CO-free solution and the voltammetric stripping stress give nearly identical values over the entire range of potentials examined. They represent two independent measurements of the same CO adlayer, one measured during its formation with the second measured during its removal. The similar stress values during CO formation and removal also suggests that the Pt surface does not undergo any structural changes that might be sensitive to a surface stress measurement, at least within the resolution of these measurements, about ±0.06 N/m.

The CO coverage difference between CO-saturated and CO-free solutions can be estimated from the stress with knowledge of the stress−coverage relationship over this range of potentials. Figure 6a shows a plot of the stripping stress (from Figure 5) vs the CO coverage obtained from the corresponding stripping charge. Stress data in the hydrogen adsorption region was excluded, where the CO-induced stress seems to decrease due to the increased compressive stress of the Pt reference state. For this exercise, we assume a linear relation with a slope of −1.84 N/m. DFT calculations suggest that assuming a linear stress response is a reasonable assumption for coverages less than 0.6.[13] Applying this linear relation to the Figure 5 stress data for the potentiostatic pulses in the CO-saturated electrolyte allows us to estimate the CO coverage as a function of potential for the CO-saturated electrolyte and compare with the experimental values for the CO-free electrolyte, as shown in Figure 6b. The solid lines are simply a guide for the eye. The stress data suggests that high CO coverage can be maintained at more positive potentials when the CO adlayer is in equilibrium with the CO-saturated electrolyte, whereas the coverage falls off at more negative

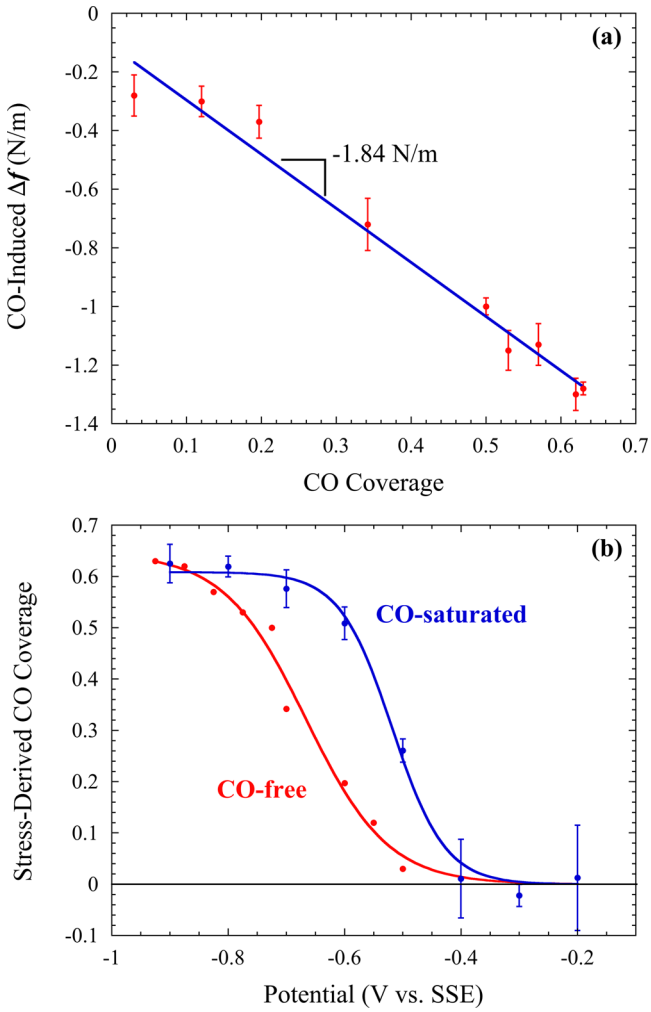

Figure 6. (a) CO-induced stress (Δf) measured during CO stripping as a function of CO surface coverage. The coverage was determined from CO stripping charge using eq 5 while the stripping stress (Δf) was taken from Figure 5. (b) Coverage vs potential plot for the CO-saturated electrolyte calculated from the Figure 5 stress values from potentiostatic pulses, using the linear relationship in panel (a). The CO-free coverage was taken from panel (a). The solid lines are only a guide for the eye.

potential when CO is absent from solution. The difference in the equilibrium CO coverage that Cuesta[51] measured as a function of the CO partial pressure in 0.1 mol/L H_2SO_4 at E_{ads} = 0.1 V vs RHE appears to be significantly increased at the more positive adsorption potentials where CO can be oxidized from the surface.

We have experimentally shown that the adsorption of CO onto (111)-textured Pt cantilever electrodes generates a compressive change in the surface stress. The magnitude of the stress change correlates first order with the CO coverage and, within the detection limits of the stress measurement, is elastically reversible. Similar levels of compressive stress have been measured for CO on Pt, adsorbed both electrochemically[13,14] and from the gas phase.[15] In addition, first-principles calculations also predict significant compressive stress associated with CO adsorption onto Pt.[13,16]

3.4. Computational Predictions of CO Adsorption onto Pt. Adsorbate-induced surface stress is often discussed in terms of charge transfer between the adsorbed species and the

https://doi.org/10.1021/acs.jpcc.2c00134
J. Phys. Chem. C 2022, 126, 4446−4457

metal surface, resulting in a bond strength change in the metal.[53−55] In that strict context, the large compressive stress that results from CO's adsorption onto a Pt surface is unexpected given that it is a charge neutral process.[12] If one considers the stress change expected from species that CO displaces from the surface, the displacement of anions would result in a negative charge and tensile stress since experimental evidence to date suggests that anions have a negative stress-charge coefficient.[56,57] The displacement of adsorbed hydrogen would result in a positive charge yet also cause tensile stress since hydrogen has a positive stress-charge coefficient on Pt.[19,21,58] Neither of these explain the observed compressive stress measured for CO adsorption. However, one proposed mechanism that accounts for compressive stress is the Blyholder model where the bonding is derived from two contributions: 5σ donation and 2π back-donation.[5,9−11,59] The 5σ orbital, which is completely filled in the gas phase, becomes partially empty, while the originally empty 2π orbitals become partially filled. Although there is significant electron interaction between the CO on the surface with the metal bands of the Pt, the net charge transfer is quite low. Molecular orbital (MO) theory supports the notion that CO adsorbs as a neutral molecule; however, the electronic structure of the CO molecule is changed considerably through orbital mixing within the metal and CO orbitals.[9]

DFT calculations[13] yield a CO adsorption stress of −4.40 N/m for θ = 0.68 and −2.22 N/m for θ = 0.50,[13] the latter being fairly close to experimental values of −2.6 N/m for similar coverage in UHV.[15] Ha et al. proposed that the compressive stress for CO adsorption can be due to charge redistribution, which lowers the tensile stress inherent to the clean Pt surface, citing the Blyholder model, as additional charge can be transferred from the Pt to the CO (2π back-donation). However, the 5σ donation from the CO to the Pt, which should result in tensile stress, was not discussed. Density-of states-calculations of Lin et al.[59] suggest that the back-donation from Pt to CO 2π orbitals dominates the binding of Pt−CO, while the σ donation from CO to Pt is less important in this binding. However, their calculations also show that after CO adsorption, the Fermi level of Pt has been shifted negatively, meaning that there has been a net transfer of electrons from Pt to CO. This is consistent with experimental results showing that the work function of the Pt surface, when covered with CO, increases by about 0.40 eV.[60−62]

We propose another explanation for the negative change in stress upon CO adsorption: the redistribution of electrons from the Pt bound to the CO to the second atomic layer of Pt atoms. We explored this possibility through DFT simulations of a CO molecule approaching a Pt surface for a CO surface coverage of 1/4 monolayer (ML). The CO distance from the surface gives us an additional parameter to explore the relationship between the charge distribution and the surface stress. In the absence of CO, we calculate a surface stress value for Pt(111) of + 4.79 N/m. This intrinsic tensile stress of clean metal surfaces is due to redistribution of the charge from the undercoordinated Pt at the surface and consequent increased bond strength between surface atoms.[54] As CO is moved toward the Pt surface, this excess tensile stress decreases approximately linearly (for short distances), as shown in Figure 7. We calculate a stress change of −1.65 N/m for a CO coverage of 1/4 ML. This is consistent with the −1.55 N/m value calculated by Ha et al. for similar CO coverage.[13]

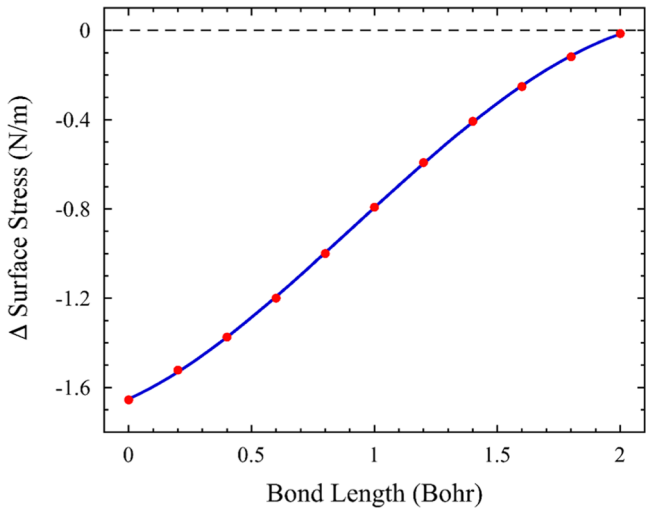

Figure 7. Computed surface stress relative to that of bare Pt is reported for Pt with a 0.25 ML coverage of CO. The "bond length" label refers to the Pt−CO distance, where 0 is the equilibrium-bonded Pt−CO. The curve serves as a guide for the eye.

Our calculations also show that when CO approaches the Pt surface, the CO polarization increases, with electron density shifting from the C to the O. However, the sum of C and O Bader charge only changes slightly, as shown in Figure 8a. This is consistent with the experimental observation that CO adsorbs as a neutral molecule. In addition to CO polarization, the charge is redistributed between the top two layers of the Pt (Figure 8b,c). Specifically, the Bader charges in the first and second layers of Pt change the most for the directly bonded atom (Pt_a^1) and its nearest neighbors in the second layer (the three Pt_a^2). The three equivalent bare Pt atoms adjacent to Pt_a^1 in the top layer (Pt_b^1) and Pt_b^2 in the second layer change very little (also shown in Figure 8b). The CO binding causes a decrease in the electron density immediately at the bonded Pt_a^1 and an increase in the nearest Pt atoms in layer two, Pt_a^2. This redistribution of electron density from the CO-bonded Pt in the top layer to its nearest neighbors in the second layer can account for the observed stress change. This can be seen in Figure S5, which shows the linear relationship between the calculated stress and Bader charge of the Pt_a^1. Although Ibach's charge redistribution model typically considers charge transfer associated with bond formation between the adsorbate and substrate,[54] our calculations show that adsorbate-induced charge redistribution within the substrate can give rise to similar changes in surface stress.

4. CONCLUSIONS

CO oxidation on Pt has been extensively studied but there is still an incomplete understanding behind the origin of compressive stress that results from the adsorption of CO on Pt. Manipulation of the CO behavior on metal surfaces to advance renewable technologies like ethanol or methanol fuel cells relies on descriptors that originate from robust fundamental explanation. This report highlights the dynamics between Pt and CO within the onset potential window for CO oxidation. Within this window, the coverage of CO on a (111)-textured Pt surface is extremely sensitive to the concentration of CO in solution, demonstrating a difference in the coverage of ≈0.3 equivalent to ≈0.5 N/m in stress at −0.6 V between saturated CO and CO-free solution. Furthermore, DFT

https://doi.org/10.1021/acs.jpcc.2c00134
J. Phys. Chem. C 2022, 126, 4446−4457

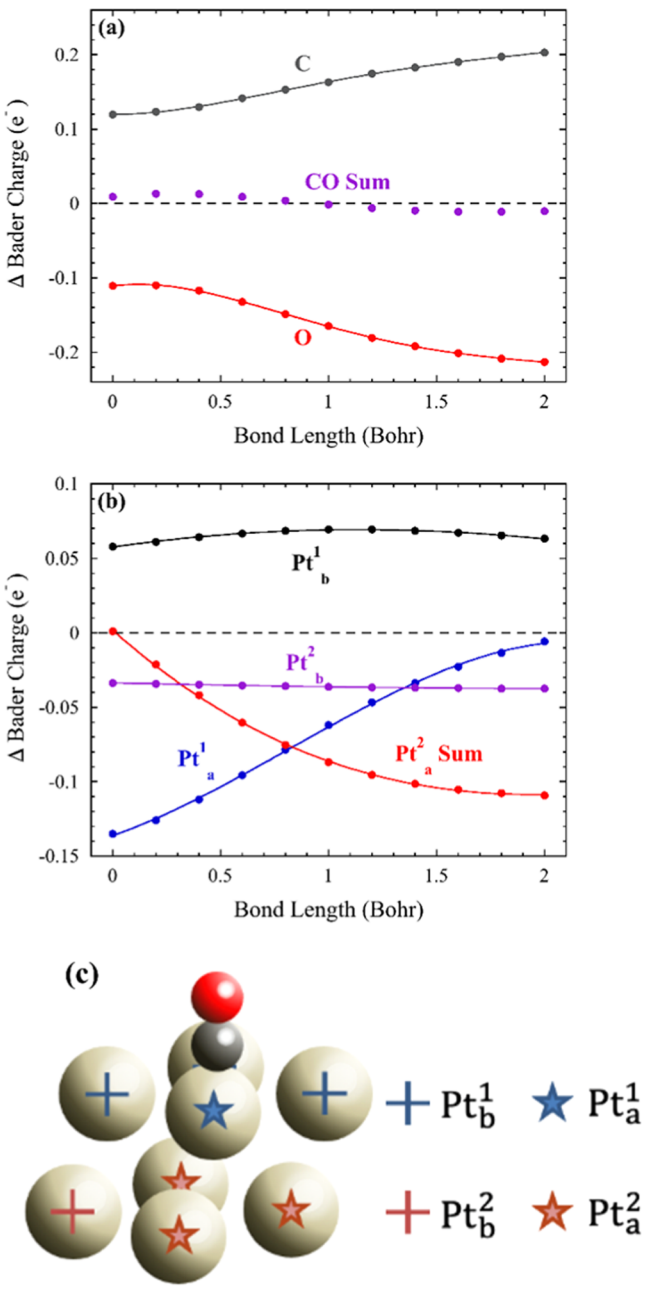

Figure 8. (a, b) Change in Bader charge from the integer value of formal charge as CO is displaced from the surface. The "bond length" label refers to the Pt−CO distance, where 0 is the equilibrium-bonded Pt−CO. (c) Pt atoms in the top layer of the unit cell (Pt^1) include one bound to CO (Pt^1_a) and three equivalent bare Pt (Pt^1_b). In the bottom layer (Pt^2), three equivalent Pt (Pt^2_a) are nearest neighbors to Pt^1_a, while Pt^2_b is not. The curves serve as guides for the eye.

calculations show that the compressive stress induced by CO is coincident with electron redistribution from the CO-bound Pt atom to the second layer of Pt atoms. Subsequent experiments using thin atomic layers of Pt on secondary metal surfaces can test the validity of this model and further refine the charge redistribution mechanism proposed. These and subsequent findings will serve as a benchmark for exploration and measurement of stress dynamics occurring at model catalytic interfaces used in alcohol-powered fuel cells, and guide the design of more efficient fuel cell catalysts.

■ ASSOCIATED CONTENT

Supporting Information

The Supporting Information is available free of charge at https://pubs.acs.org/doi/10.1021/acs.jpcc.2c00134.

Cyclic voltammogram of Pt in Ar-saturated 0.1 M $KHCO_3$ with X-ray diffraction pattern of sputtered Pt, details on determining the uncertainty in curvature measurements due to gas bubbling with plotted results, stripping voltammograms for a Pt surface exposed to CO at −0.55 V, a plot demonstrating the relationship between $-q_{dis}$ and potential used to determine CO coverage using eq 5, and a plot showing the calculated relationship between Bader charge and surface stress (PDF)

■ AUTHOR INFORMATION

Corresponding Author

David Raciti − *Material Measurement Laboratory, National Institute of Standards and Technology, Gaithersburg, Maryland 20899, United States;* orcid.org/0000-0002-9580-4524; Email: david.raciti@nist.gov

Authors

Kathleen A. Schwarz − *Material Measurement Laboratory, National Institute of Standards and Technology, Gaithersburg, Maryland 20899, United States;* orcid.org/0000-0002-1539-4511

John Vinson − *Material Measurement Laboratory, National Institute of Standards and Technology, Gaithersburg, Maryland 20899, United States;* orcid.org/0000-0002-7619-7060

Gery R. Stafford − *Material Measurement Laboratory, National Institute of Standards and Technology, Gaithersburg, Maryland 20899, United States*

Complete contact information is available at: https://pubs.acs.org/10.1021/acs.jpcc.2c00134

Notes

The authors declare no competing financial interest.

■ ACKNOWLEDGMENTS

The authors gratefully acknowledge Carlos Beauchamp, Maureen Williams, and Eric Rus for technical contributions. Cantilever metallization was performed at the Center for Nanoscale Science and Technology NanoFab at the National Institute of Standards and Technology. D.R. acknowledges support from the National Research Council Postdoctoral Fellowship Program.

■ ADDITIONAL NOTE

[#]Certain trade names are mentioned for experimental information only; in no case does it imply a recommendation or endorsement by NIST.

■ REFERENCES

(1) Alsarhan, L. M.; Alayyar, A. S.; Alqahtani, N. B.; Khdary, N. H. Circular Carbon Economy (CCE): A Way to Invest CO_2 and Protect the Environment, a Review. *Sustainability* **2021**, *13*, 11625.

(2) Tan, E. C. D.; Lamers, P. Circular Bioeconomy Concepts—a Perspective. *Front. Sustainability* **2021**, *2*, No. 701509.

(3) García, G.; Koper, M. T. Carbon Monoxide Oxidation on Pt Single Crystal Electrodes: Understanding the Catalysis for Low Temperature Fuel Cells. *ChemPhysChem* **2011**, *12*, 2064−2072.
(4) Cuesta, A.; Gutierrez, C. *CO Adsorption on Platinum Electrodes*; John Wiley & Sons, Inc., 2011.
(5) Föhlisch, A.; Nyberg, M.; Bennich, P.; Triguero, L.; Hasselstrom, J.; Karis, O.; Pettersson, L. G. M.; Nilsson, A. The Bonding of CO to Metal Surfaces. *J. Chem. Phys.* **2000**, *112*, 1946.
(6) Toyoshima, I.; Somorjai, G. A. Heats of Chemisorption of O_2, H_2, CO, CO_2, and N_2 on Polycrystalline and Single Crystal Transition Metal Surfaces. *Catal. Rev.: Sci. Eng.* **1979**, *19*, 105−159.
(7) Marković, N. M.; Grgur, B. N.; Lucas, C. A.; Ross, P. N. Surface Chemistry of CO on Pt(100)-Bimetallic Surfaces: Displacement Effects. *Langmuir* **2000**, *16*, 1998.
(8) Orts, J. M.; Gomez, R.; Feliu, J. M.; Aldaz, A.; Clavilier, J. Potentiostatic Charge Displacement by Exchanging Adsorbed Species on Pt(111) Electrodes-Acidic Electrolytes with Specific Anion Adsorption. *Electrochim. Acta* **1994**, *39*, 1519.
(9) Aizawa, H.; Tsuneyuki, S. First-Principles Study of CO Bonding to Pt(111): Validity of the Blyholder Model. *Surf. Sci.* **1998**, *399*, L364.
(10) Blyholder, G. Molecular Orbital View of Chemisorbed Carbon Monioxide. *J. Phys. Chem. A* **1964**, *68*, 2772.
(11) Grinberg, I.; Yourdshahyan, Y.; Rappe, A. M. CO on Pt(111) Puzzle: A Possible Solution. *J. Chem. Phys.* **2002**, *117*, 2264.
(12) Clavilier, J.; Albalat, R.; Gomez, R.; Orts, J. M.; Feliu, J. M. Displacement of Adsorbed Iodine on Platinum Single-Crystal Electrodes by Irreversible Adsorption of CO at Controlled Potential. *J. Electroanal. Chem.* **1993**, *360*, 325.
(13) Ha, Y.; Zeng, Z.; Cohen, Y.; Greeley, J.; Gewirth, A. Electrochemical Surface Stress Development During CO and NO Oxidation on Pt. *J. Phys. Chem. C* **2016**, *120*, 8674.
(14) Mickelson, L.; Heaton, T.; Friesen, C. Surface Stress Observations During the Adsorption and Electrochemical Oxidation of CO on Pt(111). *J. Phys. Chem. C* **2008**, *112*, 1060.
(15) Grossmann, A.; Erley, W.; Ibach, H. Adsorbate-Induced Surface Stress Measurements: A New Method for Monitoring in Situ Surface Reactions. *Surf. Rev. Lett.* **1995**, *02*, 543.
(16) Brako, R.; Sokcevic, D. Adsorbate-Induced Substrate Relaxation and the Adsorbate-Adsorbate Interaction. *Surf. Sci.* **2000**, *469*, 185.
(17) Ibach, H. The Role of Surface Stress in Reconstruction, Epitaxial Growth and Stabilization of Mesoscopic Structures. *Surf. Sci. Rep.* **1997**, *29*, 195−263.
(18) Feibelman, P. J. First-Principles Calculations of Stress Induced by Gas Adsorption on Pt(111). *Phys. Rev. B* **1997**, *56*, 2175.
(19) Weissmüller, J.; Viswanath, R. N.; Kibler, L. A.; Kolb, D. M. Impact of Surface Mechanics on the Reactivity of Electrodes. *Phys. Rev. Lett.* **2011**, *13*, 2114.
(20) Smetanin, M.; Deng, Q.; Weissmuller, J. Dynamic Electro-Chemo-Mechanical Analysis During Cyclic Voltammetry. *Phys. Rev. Lett.* **2011**, *13*, 17313−17322.
(21) Lafouresse, M. C.; Bertocci, U.; Stafford, G. R. Dynamic Stress Analysis Applied to (111)-Textured Pt in $HClO_4$ Electrolyte. *J. Electrochem. Soc.* **2013**, *160*, H636−H643.
(22) Stafford, G. R.; Kongstein, O. E.; Haarberg, G. M. In Situ Stress Measurements During Aluminum Deposition from $AlCl_3$-EtMeImCl Ionic Liquid. *J. Electrochem. Soc.* **2006**, *153*, C207−C212.
(23) Vaudin, M. D. Crystallographic Texture in Ceramics and Metals. *J. Res. Natl. Inst. Stand. Technol.* **2001**, *106*, 1063−1069.
(24) Stoney, G. G. The Tension of Metallic Films Deposited by Electrolysis. *Proc. R. Soc. London, Ser. A* **1909**, *82*, 172−175.
(25) Kongstein, O. E.; Bertocci, U.; Stafford, G. R. In Situ Stress Measurements During Copper Electrodeposition on (111)-Textured Au. *J. Electrochem. Soc.* **2005**, *152*, C116−C123.
(26) Stafford, G. R.; Bertocci, U. In Situ Stress and Nanogravimetric Measurements During Underpotential Deposition of Bismuth on (111)-Textured Au. *J. Phys. Chem. B* **2006**, *110*, 15493−15498.
(27) Xu, D.; Sriram, V.; Ozolins, V.; Yang, J. M.; Tu, K. N.; Stafford, G. R.; Beauchamp, C. In Situ Measurements of Stress Evolution for Nanotwin Formation During Pulse Electrodeposition of Copper. *J. Appl. Phys.* **2009**, *105*, 023521.
(28) Floro, J.; Chason, E.; Lee, S.; Twesten, R.; Hwang, R.; Freund, L. Real-Time Stress Evolution During $Si_{1-X}Ge_X$ Heteroepitaxy: Dislocations, Islanding, and Segregation. *J. Electron. Mater.* **1997**, *26*, 969−979.
(29) Frieberg, B. R.; Page, K. A.; Graybill, J. R.; Walker, M. L.; Stafford, C. M.; Stafford, G. R.; Soles, C. L. Mechanical Response of Thermally Annealed Nafion Thin Films. *Acs Appl. Mater. Interfaces* **2016**, *8*, 33240−33249.
(30) Page, K. A.; Shin, J. W.; Eastman, S. A.; Rowe, B. W.; Kim, S.; Kusoglu, A.; Yager, K. G.; Stafford, G. R. In Situ Method for Measuring the Mechanical Properties of Nafion Thin Films During Hydration Cycles. *ACS Appl. Mater. Interfaces* **2015**, *7*, 17874−17883.
(31) Perdew, J. P.; Burke, K.; Ernzerhof, M. Generalized Gradient Approximation Made Simple. *Phys. Rev. Lett.* **1996**, *77*, 3865.
(32) van Setten, M. J.; Giantomassi, M.; Bousquet, E.; Verstraete, M. J.; Hamann, D. R.; Gonze, X.; Rignanese, G.-M. The Pseudodojo: Training and Grading a 85 Element Optimized Norm-Conserving Pseudopotential Table. *Comput. Phys. Commun.* **2018**, *226*, 39−54.
(33) Giannozzi, P.; Baseggio, O.; Bonfa, P.; Brunato, D.; Car, R.; Carnimeo, I.; Cavazzoni, C.; de Gironcoli, S.; Delugas, P.; Ruffino, F. F.; et al. Quantum Espresso toward the Exascale. *J. Chem. Phys.* **2020**, *152*, No. 154105.
(34) Hamann, D. R. Optimized Norm-Conserving Vanderbilt Pseudopotentials. *Phys. Rev. B* **2013**, *88*, No. 085117.
(35) Otani, M.; Sugino, O. First-Principles Calculations of Charged Surfaces and Interfaces: A Plane-Wave Nonrepeated Slab Approach. *Phys. Rev. B* **2006**, *73*, No. 115407.
(36) Shiihara, Y.; Kohyama, M.; Ishibashi, S. Origin of Surface Stress on Late Transition Metal Surfaces: Ab Initio Local Stress and Tight-Binding Model. *Phys. Rev. B: Condens. Matter Mater. Phys.* **2013**, *87*, No. 125430.
(37) Cuesta, A.; Couto, A.; Rincon, A.; Perez, M. C.; Lopez-Cudero, A.; Gutierrez, C. Potential Dependence of the Saturation CO Coverage of Pt Electrodes: The Origin of the Pre-Peak in CO-Stripping Voltammograms. Part 3: Pt(Poly). *J. Electron. Chem.* **2006**, *586*, 184.
(38) Kanezashi, I.; Nohara, S.; Omura, J.; Watanabe, M.; Uchida, H. Electrochemical Quartz Crystal Microbalance Analysis of the CO Oxidation Reaction at Pt Alloy Electrodes. *J. Electroanal. Chem.* **2011**, *662*, 123.
(39) Somorjai, G. A. *Introduction to Surface Chemistry and Catalysis*; John Wiley & Sons: New York, 1994.
(40) Heinen, M.; Chen, Y. X.; Jusys, Z.; Behm, R. J. In Situ ATR-FTIRS Coupled with on-Line DEMS under Controlled Mass Transport Conditions—a Novel Tool for Electrocatalytic Reaction Studies. *Electrochim. Acta* **2007**, *52*, 5634−5643.
(41) Ray, N. K.; Anderson, A. B. Variations in C-O and Pt-C Frequencies for CO on a Platinum Electrode. *J. Phys. Chem. B* **1982**, *86*, 4851.
(42) Russell, J. W.; Overend, J.; Scanlon, K.; Severson, M.; Bewick, A. Infrared Spectrum of Carbon Monoxide on a Platinum Electrode in Acidic Solution. *J. Phys. Chem. C* **1982**, *86*, 3066.
(43) Schardt, B. C.; Yau, S. L.; Rinaldi, F. Atomic Resolution Imaging of Adsorbates on Metal Surfaces in Air: Iodine Adsorption on Pt(111). *Science* **1989**, *243*, 1050.
(44) Clavilier, J.; Albalat, R.; et al. Study of the Charge Displacement at Constant Potential During CO Adsorption on Pt(110) and Pt(111) Electrodes in Contact with a Perchloric Acid Solution. *J. Electroanal. Chem.* **1992**, *330*, 489−497.
(45) Climent, V.; García-Araez, N.; Herrero, E.; Feliu, J. Potential of Zero Total Charge of Platinum Single Crystals: A Local Approach to Stepped Surfaces Vicinal to Pt(111). *Russ. J. Electrochem.* **2006**, *42*, 1145.
(46) Gómez, R.; Feliu, J. M.; Aldaz, A.; Weaver, M. J. Validity of Double-Layer Charge-Corrected Voltammetry for Assaying Carbon Monoxide Coverages on Ordered Transition Metals: Comparisons

https://doi.org/10.1021/acs.jpcc.2c00134
J. Phys. Chem. C 2022, 126, 4446−4457

with Adlayer Structures in Electrochemical and Ultrahigh Vacuum Environments. *Surf. Sci.* **1998**, *410*, 48.
(47) Orts, J. M.; Fernandez-Vega, A.; Feliu, J. M.; Aldaz, A.; Clavilier, J. Electrochemical Behavior of CO Layers Formed by Solution Dosing at Open Circuit on Pt(111). Voltammetric Determination of CO Coverages at Full Hydrogen Adsorption Blocking in Various Acid Media. *Electroanal. Chem.* **1992**, *327*, 261.
(48) Podlovchenko, B. I.; Gladysheva, T. D. Variations in the Total Charge and the Open-Circuit Potential During the CO Adsorption on a Platinum Electrode in Chloride Solutions. *Russ. J. Electrochem.* **2001**, *37*, 771.
(49) Silva, C. D.; Cabello, G.; Christinelli, W. A.; Pereira, E. C.; Cuesta, A. Simultaneous Time-Resolved ATR-SEIRAS and CO-Charge Displacement Experiments: The Dynamics of CO Adsorption on Polycrystalline Pt. *J. Electron. Chem.* **2017**, *800*, 25.
(50) Gisbert, R.; Garcia, G.; Koper, M. T. M. Oxidation of Carbon Monoxide on Poly-Oriented and Single-Crystalline Platinum Electrodes over a Wide Range of pH. *Electrochim. Acta* **2011**, *56*, 2443−2449.
(51) Cuesta, A.; Perez, M. C.; Rincon, A.; Gutierrez, C. Adsorption Isotherm of CO on Pt(111) Electrodes. *ChemPhysChem* **2006**, *7*, 2346−2351.
(52) Akemann, W.; Friedrich, K. A.; Stimming, U. Potential-Dependence of CO Adlayer Structures on Pt(111) Electrodes in Acid Solution: Evidence for a Site Selective Charge Transfer. *J. Chem. Phys.* **2000**, *113*, 6864.
(53) Haiss, W. Surface Stress of Clean and Adsorbate-Covered Solids. *Rep. Prog. Phys.* **2001**, *64*, 591.
(54) Ibach, H. Adsorbate-Induced Surface Stress. *J. Vac. Sci. Technol., A* **1994**, *12*, 2240−2245.
(55) Sander, D.; Linke, U.; Ibach, H. Adsorbate-Induced Surface Stress: Sulfur, Oxygen and Carbon on Ni(100). *Surf. Sci.* **1992**, *272*, 318−325.
(56) Haiss, W.; Nichols, R. J.; Sass, J. K.; Charle, K. P. Linear Correlation between Surface Stress and Surface Charge in Anion Adsorption on Au(111). *J. Electroanal. Chem.* **1998**, *452*, 199.
(57) Viswanath, R. N.; Kramer, D.; Weissmüller, J. Variation of the Surface Stress-Charge Coefficient of Platinum with Electrolyte Concentration. *Langmuir* **2005**, *21*, 4604.
(58) Viswanath, R. N.; Kramer, D.; Weissmüller, J. Adsorbate Effects on the Surface Stress-Charge Response of Platinum Electrodes. *Electrochim. Acta* **2008**, *53*, 2757.
(59) Lin, W.-F.; Sun, S.-G.; Tian, Z.-Q.; Tian, Z.-W. Quantum Chemistry and in Situ FTIR Spectroscopy Studies on Potential-Dependent Properties of CO Adsorbed on Pt Electrodes. *Electrochim. Acta* **1993**, *38*, 1107.
(60) Behm, R. J.; Thiel, P. A.; Norton, P. R.; Ertl, G. The Interaction of CO and Pt(100). 1. Mechanism of Adsorption and Pt Phase Transition. *J. Chem. Phys.* **1983**, *78*, 7437.
(61) Comrie, C. M.; Lambert, R. M. Chemisorption and the Surface Structural Chemistry of Carbon Monoxide on Pt (110). *J. Chem. Soc., Faraday Trans. 1* **1976**, *72*, 1659−1669.
(62) Lambert, R. M. On the Interpretation of Leed Patterns Due to CO Adsorption on the (110) Faces of Ni, Pd, Pt, and Ir. *Surf. Sci.* **1975**, *49*, 325.

https://doi.org/10.1021/acs.jpcc.2c00134
J. Phys. Chem. C 2022, 126, 4446−4457